

ATPrompt: Textual Prompt Learning with Embedded Attributes

Zheng Li^{1,3}, Yibing Song^{3,4}, Penghai Zhao¹, Ming-Ming Cheng^{1,2}, Xiang Li^{1,2*}, Jian Yang^{1*}

¹ VCIP, College of Computer Science, Nankai University, ² NKIARI, Shenzhen Futian,

³ DAMO Academy, Alibaba Group, ⁴ Hupan Lab

zhengli97@mail.nankai.edu.cn, {xiang.li.implus, csjyang}@nankai.edu.cn

Project Page: [zhengli97.github.io/ATPrompt](https://github.com/zhengli97/ATPrompt)

Abstract

Textual-based prompt learning methods primarily employ multiple learnable soft prompts and hard class tokens in a cascading manner as text prompt inputs, aiming to align image and text (category) spaces for downstream tasks. However, current training is restricted to aligning images with predefined known categories and cannot be associated with unknown categories. In this work, we propose utilizing universal attributes as a bridge to enhance the alignment between images and unknown categories. Specifically, we introduce an Attribute-embedded Textual Prompt learning method for vision-language models, named **AT-Prompt**. This approach expands the learning space of soft prompts from the original one-dimensional category level into the multi-dimensional attribute level by incorporating multiple universal attribute tokens into the learnable soft prompts. Through this modification, we transform the text prompt from a category-centric form to an attribute-category hybrid form. To finalize the attributes for downstream tasks, we propose a differentiable attribute search method that learns to identify representative and suitable attributes from a candidate pool summarized by a large language model. As an easy-to-use plug-in technique, AT-Prompt can seamlessly replace the existing prompt format of textual-based methods, offering general improvements at a negligible computational cost. Extensive experiments on 11 datasets demonstrate the effectiveness of our method.

1. Introduction

Vision-Language Models (VLMs) [12, 26, 33, 37, 38], such as CLIP [33] and ALIGN [12], have demonstrated exceptional performance in recent years. These models are trained with a contrastive loss to establish alignment between image and text (category) space. Inspired by the success of NLP [21, 22], prompt learning [13, 49, 50] has

*Corresponding author.

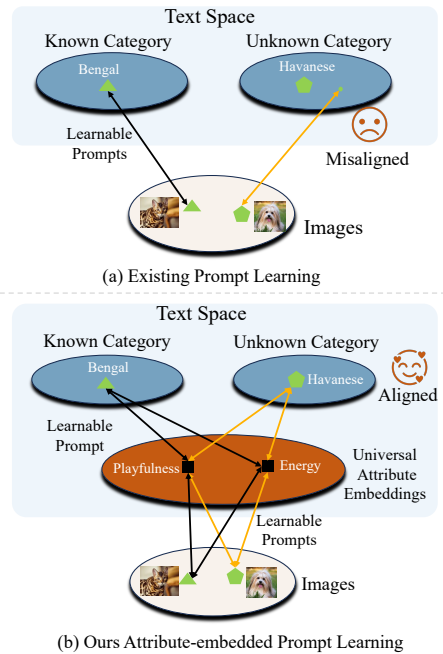


Figure 1. Comparison of image and text (category) alignment processes through learnable prompts. (a) Current prompt learning methods align images with predefined categories but fail to establish accurate associations with unknown categories. (b) ATPrompt leverages universal attributes as an intermediary to create more accurate alignments between images and unknown categories.

emerged as a parameter-efficient tool to adapt powerful VLMs to downstream tasks. Models with a few learnable soft prompt tokens can achieve performance parity with, or even outperform, fully fine-tuned ones [13]. Depending on how the soft prompt tokens are applied, existing methods can be broadly classified into textual-based [15, 16, 24, 43, 49, 50] and visual-based approaches [1, 2, 13, 19, 47]. Among these, the textual-based method is the most fundamental and straightforward, comprising the majority.

In typical image classification tasks, current text-based methods [15, 16, 49, 50] predominantly employ the traditional approach of concatenating learnable soft prompts

with hard class tokens to replace handcrafted text prompts (e.g., “a photo of a {classname}”) as inputs to the encoder. Although this text prompt demonstrates strong performance, it restricts image alignment during training to predefined known categories only, thereby preventing accurate associations with unknown categories, as shown in Fig. 1(a). Intuitively, when confronted with an unfamiliar category, humans often associate it with additional attributes (e.g., color, shape, and texture) to increase comprehensibility and clarity, rather than merely stating the object’s name. For instance, one might describe a cheetah as: “The cheetah is a cat-like animal with a *small head*, *short yellow hair*, and *black spots*,” or refer to an apple as “That *red spherical* fruit with *orange stripes* is an apple,” instead of using a general description such as “This is a cheetah” or “That fruit is an apple.”

Inspired by these observations, in this work, we propose to utilize attributes as a bridge to enhance the alignment between images and unknown categories. Specifically, we introduce an attribute-embedded textual prompt learning method for VLMs, named ATPrompt. This method extends the learning space of soft prompts from the original one-dimensional category level to the multi-dimensional attribute level by embedding multiple fixed universal attribute tokens into the learnable soft prompts. Guided by these attributes, soft prompts acquire not only category-specific but also attribute-related general representations during training, thereby enhancing the alignment between images and unknown categories compared to the original method, as shown in Fig. 1(b). Additionally, based on the depth at which soft prompts are applied, we propose two versions of ATPrompt: shallow and deep, which ensures compatibility with existing methods of varying depths [15, 16, 50]. To finalize these universal attributes, we introduce a differentiable attribute search method, which learns to identify suitable attributes from a candidate pool constructed by LLMs. Once the search is complete, the selected attributes are integrated into ATPrompt for targeted model training.

As an easy-to-use plug-in technique, ATPrompt can seamlessly substitute existing forms used in textual-based prompt learning methods, yielding general improvements with negligible additional computational overhead.

Our contributions can be summarized as follows:

- We propose a simple and effective attribute-embedded textual prompt learning method that expands the learning space of soft prompts from a one-dimensional class level to the multi-dimensional attribute level.
- For selecting embedded attributes, we design a differentiable search method that learns to select suitable attributes from a candidate pool summarized by LLMs.
- Both shallow and deep versions of ATPrompt are introduced to achieve compatibility with existing prompt learning methods of different depths.

- Extensive experiments demonstrate that ATPrompt can be seamlessly integrated into existing textual-based methods, yielding general improvements across 11 datasets with negligible additional computational costs.

2. Related Work

Prompt Learning for VLMs. Inspired by recent advancements in NLP [21, 22], prompt learning [15, 16, 24, 35, 49–51] has garnered significant interest among vision researchers aiming to apply these techniques to VLMs [12, 33], such as CLIP. CoOp [50] is the pioneering text-based approach that introduced the concept of using a combination of soft textual tokens and a hard class token as input. Subsequent studies [15, 16, 20, 24, 45, 49] have predominantly followed this textual prompt format. However, this form constrains the soft prompts to align with images within a one-dimensional, predefined category space, limiting their applicability to unknown categories. Therefore, training based on the current text form will be more likely to overfit to known categories, diminishing their zero-shot generalization capability for unknown categories. To address this limitation, several methods have been proposed [14, 16, 24, 45, 51]. For instance, KgCoOp [45] uses handcrafted hard prompts to regularize learnable soft prompts during training. PromptSRC [16] utilizes CLIP’s [33] original features to regularize the learning of soft prompts for image and text branches. PromptKD [24] utilizes a pre-trained strong teacher model to guide the learning of a student model with learnable prompts. Despite these advancements, none of the above methods address the inherent limitations of the format itself. In this work, we introduce the attribute-embedded textual prompt format for VLMs, which proposes to utilize attributes as a bridge to build more accurate associations between images and unknown categories.

Attributes for VLMs. In practice, categories typically encompass multiple attributes. When individuals encounter an unfamiliar category, they often describe it using additional attributes to enhance the clarity of their communication, rather than merely stating its name. Inspired by this observation, numerous studies [4, 28, 39, 41, 46] have begun to leverage attributes to support their objectives. VCD [28] was the pioneering work to propose the use of LLMs to decompose class names into multiple *intra-class* attributes (e.g., beak and tail for birds) for classification. ArGue [39] breaks down extensive descriptions into multiple *intra-class* attributes and trains soft prompts to align with the encoded features of these attributes. AAPL [17] introduces a meta-network to extract visual attribute features based on encoded image features, facilitating image-text alignment. Most previous studies have concentrated on utilizing *intra-class* attributes to improve model performance by providing supplementary attribute information. However, when confronted with an unknown class, it becomes

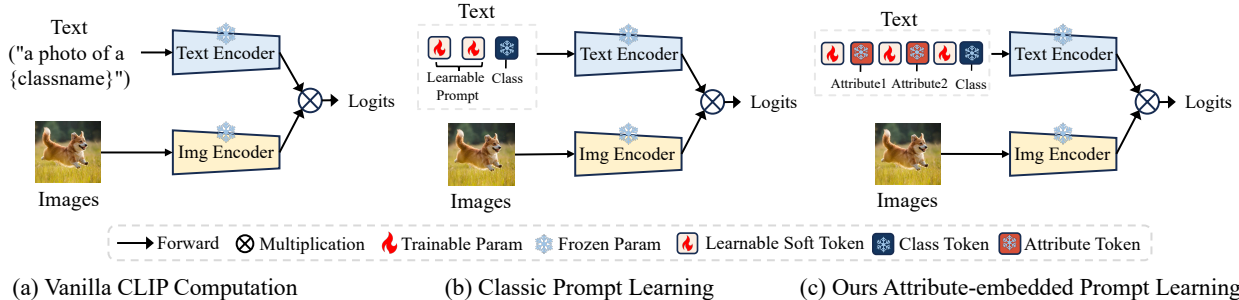


Figure 2. Architectural comparison among vanilla CLIP [33], classic prompt learning [50], and our proposed attribute-embedded prompt learning. (a) Vanilla CLIP employs a hand-crafted text template, “a photo of a {classname}”, as input to the text encoder. (b) Classical prompt learning proposes a new text form that concatenates multiple learnable soft tokens with class tokens, replacing the manually designed hard template. (c) Our ATPrompt embeds multiple fixed attribute tokens into the set of soft tokens, transforming the original form into an attribute-class mixed form for prompt learning.

necessary to reacquire the attributes of the new class—a process that is both complex and costly. In this work, we focus on using LLMs to mine universal *inter-class* attributes (e.g., color, shape, texture) for prompt learning. Instead of taking attributes as the learning objective like previous work, we propose to embed universal attributes into soft prompts, transforming the existing class-centric form [50] into a hybrid attribute-class learnable textual prompt form. Our approach can be seamlessly integrated into existing textual-based methods, enhancing their performance without incurring additional computational costs.

3. Method

Prompt learning [15, 16, 49–51] aims to enhance the generalization ability of pre-trained VLMs like CLIP on downstream tasks by training inserted learnable soft prompts. Existing textual-based methods all follow the classic prompt paradigm, concatenating soft prompt tokens and hard class tokens as the input to the encoder, as shown in Fig. 2(b). In this paper, we propose a simple and effective textual prompt learning method, named ATPrompt, which embeds multiple fixed universal attribute tokens into the original soft prompts, as shown in Fig. 2(c). Guided by these attributes, soft prompts can learn not only category-specific but also attribute-related general representations through training. When encountering unknown categories, these learned prompts can promote better image-text alignment. To determine these universal attributes, we introduce an automated pipeline consisting of multiple steps. First, we utilize LLM to summarize the attribute pool for the current downstream category. Then a differentiable attribute search method is introduced to find attributes in the pool that best suit our attribute-embedded prompt forms. Once the attributes are determined, we incorporate them into our ATPrompt for targeted model fine-tuning.

In the following, we introduce the background of VLMs and prompt learning in Sec. 3.1. Then we introduce our

attribute-embedded prompt learning method in Sec. 3.2 and the attribute search method in Sec. 3.3.

3.1. Preliminary

Vision-Language Models. Existing VLMs [12, 33], such as CLIP, have demonstrated remarkable zero-shot generalization performance after training with 400 million image-text pairs. The primary objective of these models is to learn the alignment between image and text modalities produced by each encoder. Given a labeled image classification dataset $D = \{(x, c)\}$ which includes N class labels $C = \{c_i\}_{i=1}^N$, CLIP makes predictions by calculating the cosine similarity between image features and the text features of each class. Specifically, for each input image x , it undergoes feature extraction via the image encoder $h_I(x)$ and obtains a feature vector $u = h_I(x)$. Simultaneously, for each class, a series of textual descriptions t are generated using the hand-crafted template. Then, these text descriptions are fed into the text encoder $h_T(t)$ to obtain text features $w = h_T(t)$. Finally, the output probability for image x classified to c is calculated as follows:

$$p(c|x) = \frac{\exp(\cos(u, w_c)/\tau)}{\sum_{i=1}^N \exp(\cos(u, w_i)/\tau)}. \quad (1)$$

where τ is the temperature parameter and $\cos(\cdot, \cdot)$ denotes cosine similarity.

Prompt Learning for VLMs. Instead of manually designed hard prompts for image-text alignment, which is inaccurate and inflexible, recent prompt learning works [15, 16, 45, 49, 50] like CoOp propose to learn appropriate soft textual prompts for downstream tasks. Concretely, M learnable soft tokens $[T_i]_{i=1}^M$ are concatenated with the hard class token [CLS] as the input of the text encoder, as shown in Fig. 2(b). Its form is shown as follows:

$$P_T = [T_1][T_2] \dots [T_M][CLS], \quad (2)$$

where M represents the soft prompt length. For simplicity, we omit the prefix and suffix tokens in the input.

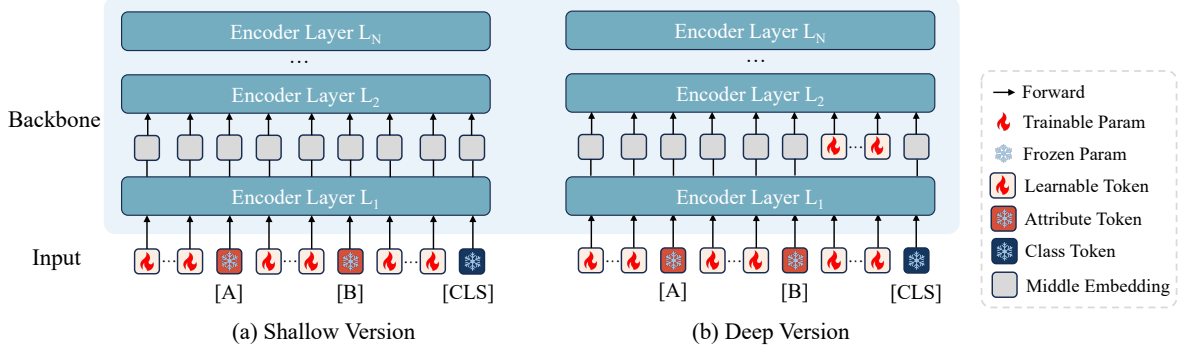


Figure 3. An illustration of the computation process for shallow and deep versions. Take two attributes [A] and [B] as examples. (a) The shallow version concatenates hard attribute tokens, soft prompt tokens, and class tokens and inputs them into the encoder for calculation. (b) The deep version uses the same input but discards the class-related soft prompt tokens after calculating the self-attention and introduces them again before the next layer. These two forms can be compatible with existing methods of varying prompt depths, including input-level ones like CoOp [50], CoCoOp [49] and depth-level ones like MaPLe [15] and PromptSRC [16].

In addition to embedding soft tokens at the input level, existing studies [13, 15, 16, 24] have also explored introducing them at deeper layers. This is achieved by adding soft tokens within the Transformer blocks and subsequently removing them after the self-attention computations. For the i -th block, this process can be described as follows:

$$[\text{CLS}_i] = L_i([\text{T}_{i-1}, \text{CLS}_{i-1}]). \quad (3)$$

where L_i represents the i -th transformer block and T_i denotes the set of learnable soft tokens, defined as $\text{T}_i = \{[T_1]_i, \dots, [T_M]_i\}$.

3.2. Learning soft prompts with universal attributes

Our approach introduces two variants, distinguished by the number of layers at which soft tokens are applied: a shallow version and a deep version, as shown in Fig. 3.

Shallow Version. We begin by introducing the shallow version, in which hard attribute tokens are incorporated solely at the input level, as illustrated in Fig. 3(a). Consider two universal attributes, A and B. According to Eqn. (2), the shallow-level text prompt P_T provided to the text encoder can be expressed as follows:

$$P_T = [T_{a_1}] \dots [T_{a_m}][A][T_{b_1}] \dots [T_{b_m}][B][T_1] \dots [T_M][\text{CLS}], \quad (4)$$

where a_m , b_m , and M are hyperparameters specifying the length of soft tokens for attributes A, B, and the class. In our method, we set these parameters to be the same by default.

Other than placing the hard class token at the end of the text prompt, we can also place it in the middle or front like:

$$P_{mid} = [T_{a_1}] \dots [T_{a_m}][A][T_1] \dots [T_M][\text{CLS}][T_{b_1}] \dots [T_{b_m}][B], \quad (5)$$

$$P_{front} = [T_1] \dots [T_M][\text{CLS}][T_{a_1}] \dots [T_{a_m}][A][T_{b_1}] \dots [T_{b_m}][B]. \quad (6)$$

In Tab. 4 we verify the performance of each position and select the best-performing end position as our default form.

Deep Version. In this version, learnable soft tokens are introduced at the input of the deep layers. Previous works, such as VPT and MaPLe, discard all soft tokens and subsequently reintroduce them after the block. When this operation is applied to attribute-related words, a gap will emerge between the introduced excessive low-level tokens and the existing high-level tokens, thereby weakening the feature continuity across layers. In this study, our approach selectively discards and then re-adds only class-related soft tokens in the input, specifically $[T_1], \dots, [T_M]$, as shown in Fig. 3(b). Based on Eqn. (3), the deep version of ATPrompt can be rewritten as follows:

$$[F_1, -, \text{CLS}_1] = L_1([\text{T}_{a_0}, A, \text{T}_{b_0}, B, \text{T}_0, \text{CLS}_0]), \quad (7)$$

$$[F_i, -, \text{CLS}_i] = L_i([F_{i-1}, \text{T}_{i-1}, \text{CLS}_{i-1}]), \quad (8)$$

$$i = 2, 3, \dots, M$$

where F_i represents the features computed by the i -th Transformer layer. We demonstrate the effectiveness of this operation in Tab. 5.

Training. Let θ represent the weight of the total soft tokens and let v denote the selected fixed attribute tokens. Training is conducted on a labeled dataset $D = \{(x, c)\}$, with the objective of minimizing the cross-entropy loss between predicted values and ground truth labels. This process can be formulated as follows:

$$\min_{\theta} L_{train} = \min_{\theta} \sum_{x \in D} CE(f(x; v, \theta), c). \quad (9)$$

where $f(\cdot)$ represents the function of the CLIP model.

3.3. Attribute search

To finalize the attributes for ATPrompt, two key aspects must be considered: selecting the appropriate content and determining the necessary quantity. A straightforward approach is to query the LLM directly. However, this method

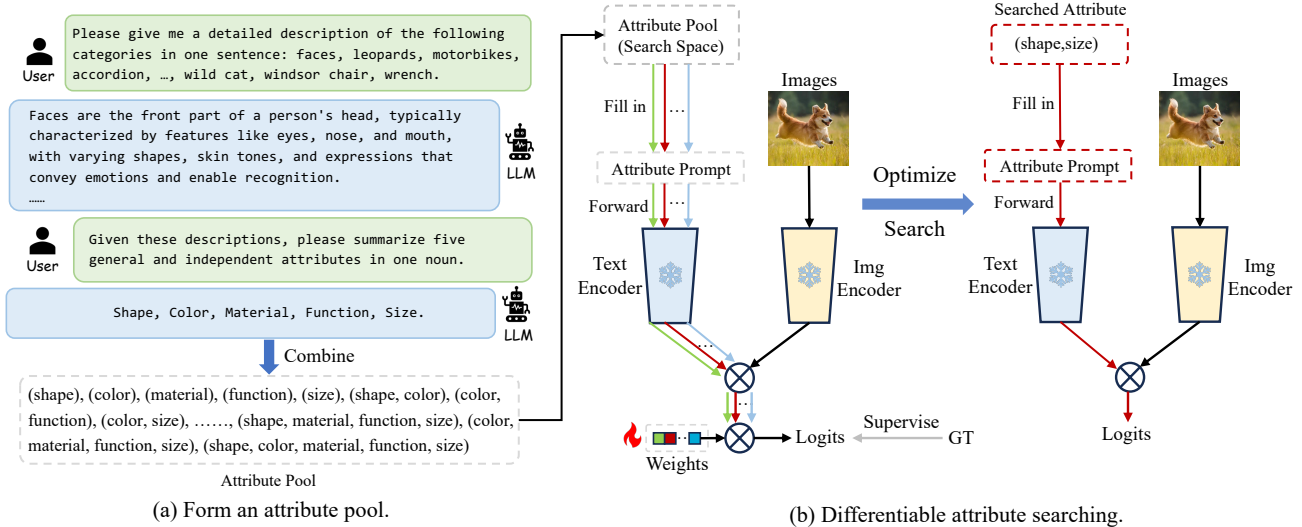


Figure 4. An overview of our attribute search pipeline. (a) We first query the LLM step by step to obtain multiple independent attributes, subsequently combining them to create an attribute pool for subsequent search methods. (b) Each colored path represents the forward computation process for a candidate in the pool. For attribute search, we propose the use of an alternating algorithm to jointly optimize soft tokens and path weights. After training, the attribute with the highest weight is selected for final use.

cannot adequately establish the optimal number of attributes for a specific downstream dataset. Additionally, without access to real data, querying solely by category name may introduce bias into the obtained attributes.

To address these challenges, we propose an automated pipeline that can select the appropriate attribute content and quantity, as illustrated in Fig. 4. Inspired by Chain-of-Thought [42, 48], we divide the entire process into multiple steps to enhance the reasoning ability of LLMs. First, we employ the LLM to generate descriptive sentences for each known category, thereby enriching category-related information. Subsequently, based on these sentences, we prompt the LLM to summarize multiple independent attribute bases across these categories. Next, an attribute pool is formed by combining different bases, as shown in Fig. 4(a). For instance, if there are five individual attribute bases, this results in 31 potential combinations of varying lengths. Note that we do not consider the attribute order specifically since it will not bring obvious semantic deviations in reality, and in the following experiments, we verify that it does not affect the final performance. We treat this pool as the search space for the following search methods.

Inspired by DARTS [25], we introduce a differentiable attribute search method that learns to find representative attributes v from the search space \mathcal{V} , as shown in Fig. 4(b). To make the search space continuous, we relax the attribute selection operation to a softmax over all possible candidates:

$$f(x, v; \alpha, \theta) = \sum_{i \in \mathcal{V}} \frac{\exp(\alpha_i)}{\sum_{i' \in \mathcal{V}} \exp(\alpha_{i'})} f(x, v_i; \theta). \quad (10)$$

where α_i represents the weight for attribute v_i . The task of

attribute search then reduces to learning the weight vector α for each attribute in the candidate pool.

After relaxation, our goal is to jointly learn the attribute weight α and soft prompt tokens θ . Same as [25, 32, 52], we use the validation set performance as the reward for the current search process and optimize the weight vector with validation loss L_{val} . The soft prompt tokens are obtained by minimizing the training loss L_{train} .

We apply the alternating algorithm [11, 23] to solve this problem, fixing one set of variables and solving for the other set. Formally, we can alternate between solving these two subproblems:

$$\hat{\alpha} = \arg \min_{\alpha} L_{val}(f(x, v; \alpha, \hat{\theta}), c), \quad (11)$$

$$\hat{\theta} = \arg \min_{\theta} L_{train}(f(x, v; \hat{\alpha}, \theta), c). \quad (12)$$

where L_{train} and L_{val} uses cross-entropy as the loss function. At the end of the search, an attribute can be selected from the ones with the highest weights.

Overall. The entire process comprises two steps. The first step is the attribute search stage. For downstream data, the attribute pool \mathcal{V} is initially formed by LLMs. Subsequently, the attribute search method is conducted within this pool to identify the attribute v that best suits our form. After the search is complete, the selected attributes are integrated into ATPrompt for targeted model training.

4. Experiments

4.1. Settings

Base-to-Novel Generalization. Following [16, 24, 49, 50], we split the dataset into base and novel classes. The model

Version		Shallow		Shallow		Shallow		Deep		Deep	
Dataset	Metric (%)	CoOp	+ATP	CoCoOp	+ATP	KgCoOp	+ATP	MaPLe	+ATP	PromptSRC	+ATP
Avg.	Base	82.69	82.68	80.47	81.69	80.73	80.96	82.28	82.90	84.26	84.30
	Novel	63.22	68.04	71.69	74.54	73.60	74.45	75.14	75.63	76.10	76.45
	HM	71.66	74.65	75.83	77.95	77.00	77.57	78.55	79.10	79.97	80.18
	Δ	-	(+2.99)	-	(+2.12)	-	(+0.57)	-	(+0.55)	-	(+0.21)
Image Net	Base	76.47	76.27	75.98	76.43	75.83	76.69	76.66	76.94	77.60	77.69
	Novel	67.88	70.60	70.43	70.50	69.96	69.74	70.54	70.72	70.73	70.83
	HM	71.92	73.33	73.10	73.35	72.78	73.05	73.47	73.70	74.01	74.10
	Δ	-	(+1.41)	-	(+0.25)	-	(+0.27)	-	(+0.23)	-	(+0.09)
Caltech 101	Base	98.00	97.95	97.96	97.96	97.72	97.87	97.74	98.15	98.10	98.23
	Novel	89.81	93.63	93.81	95.27	94.39	95.09	94.36	94.94	94.03	94.91
	HM	93.73	95.74	95.84	96.60	96.03	96.46	96.02	96.52	96.02	96.54
	Δ	-	(+2.01)	-	(+0.76)	-	(+0.43)	-	(+0.50)	-	(+0.52)
Oxford Pets	Base	93.67	94.77	95.20	95.46	94.65	94.92	95.43	95.91	95.33	95.64
	Novel	95.29	96.59	97.69	97.89	97.76	97.72	97.76	97.54	97.30	97.43
	HM	94.47	95.67	96.43	96.66	96.18	96.30	96.58	96.72	96.30	96.53
	Δ	-	(+1.20)	-	(+0.23)	-	(+0.12)	-	(+0.14)	-	(+0.23)
Stanford Cars	Base	78.12	77.43	70.49	74.50	71.76	72.36	72.94	74.85	78.27	79.25
	Novel	60.40	66.55	73.59	73.47	75.04	74.98	74.00	73.70	74.97	74.95
	HM	68.13	71.58	72.01	73.98	73.36	73.65	73.47	74.27	76.58	77.04
	Δ	-	(+3.45)	-	(+1.97)	-	(+0.29)	-	(+0.80)	-	(+0.46)
Flowers 102	Base	97.60	97.44	94.87	96.52	95.00	94.05	95.92	97.66	98.07	97.82
	Novel	59.67	67.52	71.75	73.59	74.73	74.61	72.46	74.47	76.50	77.02
	HM	74.06	79.77	81.71	83.51	83.65	83.21	82.56	84.50	85.95	86.18
	Δ	-	(+5.71)	-	(+1.80)	-	(-0.44)	-	(+1.94)	-	(+0.23)
Food 101	Base	88.33	88.74	90.70	90.59	90.50	90.54	90.71	90.58	90.67	90.77
	Novel	82.26	87.44	91.29	91.74	91.70	91.79	92.05	91.94	91.53	91.78
	HM	85.19	88.09	90.99	91.16	91.09	91.16	91.38	91.25	91.10	91.27
	Δ	-	(+2.90)	-	(+0.17)	-	(+0.07)	-	(-0.13)	-	(+0.17)
FGVC Aircraft	Base	40.44	40.38	33.41	37.30	36.21	35.59	37.44	37.61	42.73	42.47
	Novel	22.30	27.22	23.71	33.15	33.55	33.41	35.61	36.15	37.87	37.01
	HM	28.75	32.52	27.74	35.10	34.83	34.47	36.50	36.87	40.15	39.55
	Δ	-	(+3.77)	-	(+7.36)	-	(-0.35)	-	(+0.37)	-	(-0.60)
SUN 397	Base	80.60	80.84	79.74	80.50	80.29	80.09	80.82	80.96	82.67	82.73
	Novel	65.89	68.64	76.86	76.86	76.53	77.22	78.70	78.11	78.47	78.64
	HM	72.51	74.24	78.27	78.64	78.36	78.63	79.75	79.51	80.52	80.63
	Δ	-	(+1.73)	-	(+0.37)	-	(+0.27)	-	(-0.24)	-	(+0.11)
DTD	Base	79.44	80.83	77.01	78.63	77.55	78.30	80.36	80.33	83.37	83.22
	Novel	41.18	45.49	56.00	56.89	54.99	55.32	59.18	57.85	62.97	62.68
	HM	54.24	58.22	64.85	66.02	64.35	64.83	68.16	67.26	71.75	71.50
	Δ	-	(+3.98)	-	(+1.17)	-	(+0.48)	-	(-0.90)	-	(-0.25)
Euro SAT	Base	92.19	90.34	87.49	87.95	85.64	88.27	94.07	94.84	92.90	92.29
	Novel	54.74	59.79	60.04	74.15	64.34	71.27	73.23	77.59	73.90	76.42
	HM	68.69	71.96	71.21	80.46	73.48	78.86	82.35	85.35	82.32	83.61
	Δ	-	(+3.27)	-	(+9.25)	-	(+5.38)	-	(+3.00)	-	(+1.29)
UCF 101	Base	84.69	84.49	82.33	82.74	82.89	81.84	83.00	84.08	87.10	87.15
	Novel	56.05	64.96	73.45	76.40	76.67	77.84	78.66	78.88	78.89	79.23
	HM	67.46	73.45	77.64	79.44	79.65	79.79	80.77	81.40	82.74	83.00
	Δ	-	(+5.99)	-	(+1.80)	-	(+0.14)	-	(+0.63)	-	(+0.26)

Table 1. Base-to-novel generalization experiments of five baselines with and without our ATPrompt on 11 recognition datasets. HM: Harmonic Mean. Δ : HM improvement of ATPrompt over previous results. “ATPrompt” is abbreviated as “ATP”. Our method achieves consistent average performance improvement over different baselines.

is trained on the base class training set and evaluated on the test set. The attributes applied in this experiment are searched based on the base class. For datasets not including validation sets, such as ImageNet, we evenly divide the available 16-shot data, allocating half for training and the remaining half for attribute search.

Cross-dataset Experiments. Same as previous works [16, 49, 50], we first train a model on source dataset (ImageNet-1K) and then evaluate on out-of-distribution datasets to test generalization performance. The attributes adopted in this experiment are searched based on the source dataset.

Attribute Search. We select five independent attributes as

Version	Method	Source		Target Dataset											Avg.	Δ
		Image Net	Caltech 101	Oxford Pets	Stanford Cars	Flowers 102	Food 101	FGVC Aircraft	SUN 397	DTD	Euro SAT	UCF 101				
Shallow	CoOp	71.51	93.70	89.14	64.51	68.71	85.30	18.47	64.15	41.92	46.39	66.55	63.88	-		
	+ATPrompt	71.67	93.96	90.65	65.01	70.40	85.86	20.97	65.77	43.44	46.59	69.92	65.26	(+1.38)		
Shallow	CoCoOp	71.02	94.43	90.14	65.32	71.88	86.06	22.94	67.36	45.73	45.37	68.21	65.74	-		
	+ATPrompt	71.27	93.79	90.62	65.90	71.17	86.03	23.22	66.63	44.44	48.70	70.71	66.59	(+0.85)		
Deep	MaPLe	70.72	93.53	90.49	65.57	72.23	86.20	24.74	67.01	46.49	48.06	68.69	66.30	-		
	+ATPrompt	70.69	94.04	91.03	66.06	71.99	86.33	24.42	67.05	45.21	48.63	69.15	66.75	(+0.45)		

Table 2. Cross-dataset generalization experiments of three baselines with and without our ATPrompt on 11 datasets. Our method achieves consistent average performance improvements over three baseline methods.

Dataset	Attribute Bases	Searched Results
ImageNet	color, size, shape, habitat, behavior	(color, shape)
Caltech101	shape, color, material, function, size	(shape, size)
OxfordPets	loyalty, affection, energy, playfulness, intelligence	(playfulness, energy)
StanfordCars	design, engine, performance, luxury, color	(luxury)
Flowers102	color, flower, habitat, growth, season	(color, habitat, growth)

Table 3. Part of the results obtained after differentiable attribute search. Please refer to the appendix for the complete results.

the basis in the attribute pool. We do not particularly consider the order of attributes, as the following experiments verify that it will not significantly affect the training results. Therefore, for five attributes, we have 31 attribute combinations as candidates for search. We use ChatGPT-4o for attribute queries. Note that our proposed attribute search process does not take days like the traditional NAS method. Since there are very few parameters to be trained in this method, the search process only takes about 40 minutes on a V100 GPU for a dataset like Caltech101. In Tab. 3, we report a subset of the attribute bases queried from the LLM and the results obtained after searching. In the appendix, we show the specific weights learned for each candidate after the search process.

Implementation Details. We evaluate the effectiveness of our method on 11 recognition datasets, including ImageNet-1K [6], Caltech-101 [7], OxfordPets [30], StanfordCars [18], Flowers-102 [29], Food-101 [3], FGVC Aircraft [27], SUN-397 [44], DTD [5], EuroSAT [8] and UCF-101 [36]. The ViT-B/16 CLIP is selected as our default model. We report base and novel class accuracy and their harmonic mean (HM) averaged over 3 runs. Please refer to the Appendix for more experimental details.

4.2. Base-to-Novel Generalization

As demonstrated in Tab. 1, we evaluate the base-to-novel generalization performance of five baseline methods, both with and without integrating ATPrompt, across 11 recogni-

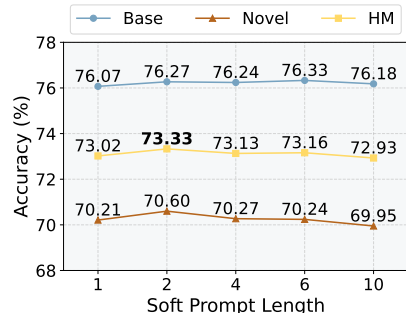


Figure 5. Illustration of varying soft token length on ImageNet. Increased tokens can lead to overfitting to the base class and weaken generalization to the novel class.

tion datasets. Notably, ATPrompt consistently enhances the average performance over all baseline methods.

Reasons for Limited Improvement in Some Conditions.

- (1) When we implement our method, we do not carefully adjust the hyperparameters of the baseline (e.g., learning rate, training epochs, loss hyperparameters); they remain consistent with the original method.
- (2) Recent advanced methods have integrated a variety of modules and regularization techniques (e.g., KG loss in KgCoOp, GPA, and SCL in PromptSRC). These additions may render the improvements introduced by our ATPrompt less perceptible or potentially redundant alongside existing enhancements.
- (3) Performance fluctuations due to limited training data.

4.3. Cross-dataset Evaluation

Tab. 2 shows the cross-dataset generalization results for three baseline methods. Our method demonstrates superior performance, with improvements of 1.38%, 0.85% and 0.45% for CoOp, CoCoOp and MaPLe respectively.

4.4. Further Analysis

In this section, we conduct ablation experiments to evaluate the operations and hyperparameters of ATPrompt, thereby validating its effectiveness. By default, the experiments are conducted on the ImageNet. To minimize the influence of other components, we mainly adopt CoOp as the baseline method. Two attributes are used in our ATPrompt. For more

experimental results, please refer to the Appendix.

Soft Prompt Length. In Fig. 5, we examine the optimal number of soft tokens for attribute and class tokens, respectively. By varying the length from 1 to 10, we can observe that introducing more soft tokens weakens the effect of embedded attribute tokens and reduces the generalization performance for unknown classes.

Class Token Position. Since our method introduces a new textual prompts format, the relative positioning of attribute tokens and class tokens requires careful consideration. In Tab. 4, we examine configurations where the class token is positioned in the middle or on either side of two attribute tokens. The results demonstrate that optimal performance is achieved when the class token is placed at the end, which aligns with the conclusions of CoOp.

Position	Base	Novel	HM
Front	76.12	70.50	73.20
Middle	76.13	70.29	73.09
End	76.27	70.60	73.33

Table 4. Comparison of different class token positions on ImageNet. The end position works best.

Prompt Operation of Deep Version. In ATPrompt-Deep, we exclusively drop class soft tokens while retaining both hard and soft attribute tokens after they pass through the block. In this part, we compare the performance of partial drop (i.e., removing attribute soft tokens while retaining hard tokens) and full drop (i.e., removing both attribute soft and hard tokens) operations, as illustrated in Tab. 5.

Operation of Attribute Token	Base	Novel	HM
Retain all hard and soft tokens	76.94	70.72	73.70
Partial drop and re-add	76.87	70.44	73.51
Full drop and re-add	76.83	70.10	73.31

Table 5. Comparison of operations on deep soft and hard attribute tokens based on MaPLE+ATPrompt. Preserving hard and soft attribute tokens in deep layers performs better than other operations.

The results show that maintaining the attributes of both hard and soft tokens during the forward process results in optimal performance. Conversely, the actions of discarding and reintroducing attribute tokens diminish the model’s effectiveness. A possible explanation for this is that such operations disrupt the continuity of attribute representations across layers and amplify the disparity with existing tokens, thereby complicating the training of soft tokens.

Attribute Order. In this study, we do not specifically focus on the order of attributes in ATPrompt because varying the sequence usually does not result in semantic deviations in reality. For example, phrases like “a yellow round leaf” and “a round yellow leaf” convey the same meaning. Tab. 6 quantitatively assesses the impact of attribute order

on prompt learning performance. From this table, we observe that despite variations in order, similar results are consistently produced, and the performance fluctuations across different orders remain within a reasonable range.

Attributes	Base	Novel	HM
(shape, color)	76.32	70.39	73.24
(color, shape)	76.27	70.60	73.33
(size, habitat)	76.44	70.23	73.20
(habitat, size)	76.46	70.16	73.14

Table 6. Comparison of different attribute orders on ImageNet. The order of attributes does not significantly affect the model, and performance fluctuations are within a reasonable range.

Comparison to Other Attributes. In Tab. 7, we explore the effectiveness of attributes derived through alternative methods, specifically by manually selecting class-irrelevant and common attributes. To highlight the comparison, we choose the fine-grained Food101 dataset for experiments.

Type	Attributes	Base	Novel	HM
Common	(shape, size)	88.48	86.87	87.67
	(color, texture)	88.50	87.17	87.83
Irrelevant	(plane, engines)	88.64	86.31	87.46
	(football, sport)	88.60	86.18	87.37
	(leather, silk)	88.56	86.82	87.68
Searched	(flavor, preparation)	88.74	87.44	88.09

Table 7. Comparison of different attributes on Food101. The attributes obtained by our method achieve the best performance.

The results indicate that manually selected irrelevant attributes exhibit comparable performance during training; however, they perform poorly when applied to new categories. This suggests that incorrect attribute tokens cause the soft tokens to develop biased representations, thereby diminishing their zero-shot generalization ability.

5. Conclusion

In this work, we propose to utilize universal attributes as a bridge to enhance the association of images and unknown categories in prompt learning. Specifically, we introduce an attribute-embedded textual prompt learning method named ATPrompt. This approach expands the learning space of soft prompts from the original one-dimensional category level into a multi-dimensional attribute level by embedding fixed universal attribute tokens into the soft prompts. To identify the appropriate attributes, we develop an automated pipeline that learns to select suitable attributes from a candidate pool summarized by LLMs. Both shallow and deep versions of ATPrompt are introduced to ensure compatibility with various existing methods. Extensive experiments demonstrate the effectiveness of our approach.

Acknowledgement. This work was supported by the Young Scientists Fund of the National Natural Science Foundation of China (Grant No.62206134), the Fundamental Research Funds for the Central Universities 070-63233084 and the Tianjin Key Laboratory of Visual Computing and Intelligent Perception (VCIP). Computation is supported by the Supercomputing Center of Nankai University (NKSC). This work was supported by the National Science Fund of China under Grant Nos. 62361166670 and U24A20330. This work was also supported by DAMO Academy through DAMO Academy Research Internship Program.

References

- [1] Hyojin Bahng, Ali Jahanian, Swami Sankaranarayanan, and Phillip Isola. Exploring visual prompts for adapting large-scale models. *arXiv preprint arXiv:2203.17274*, 2022. [1](#)
- [2] Amir Bar, Yossi Gandelsman, Trevor Darrell, Amir Globerson, and Alexei Efros. Visual prompting via image inpainting. *NeurIPS*, 35:25005–25017, 2022. [1](#)
- [3] Lukas Bossard, Matthieu Guillaumin, and Luc Van Gool. Food-101—mining discriminative components with random forests. In *ECCV*, pages 446–461. Springer, 2014. [7](#), [11](#)
- [4] Keyan Chen, Xiaolong Jiang, Yao Hu, Xu Tang, Yan Gao, Jianqi Chen, and Weidi Xie. Ovarnet: Towards open-vocabulary object attribute recognition. In *CVPR*, pages 23518–23527, 2023. [2](#)
- [5] Mircea Cimpoi, Subhansu Maji, Iasonas Kokkinos, Sammy Mohamed, and Andrea Vedaldi. Describing textures in the wild. In *CVPR*, pages 3606–3613, 2014. [7](#), [11](#)
- [6] Jia Deng, Wei Dong, Richard Socher, Li-Jia Li, Kai Li, and Li Fei-Fei. Imagenet: A large-scale hierarchical image database. In *CVPR*, pages 248–255, 2009. [7](#), [11](#)
- [7] Li Fei-Fei, Rob Fergus, and Pietro Perona. Learning generative visual models from few training examples: An incremental bayesian approach tested on 101 object categories. In *CVPR workshop*, pages 178–178. IEEE, 2004. [7](#), [11](#)
- [8] Patrick Helber, Benjamin Bischke, Andreas Dengel, and Damian Borth. Eurosat: A novel dataset and deep learning benchmark for land use and land cover classification. *IEEE Journal of Selected Topics in Applied Earth Observations and Remote Sensing*, 12(7):2217–2226, 2019. [7](#), [11](#)
- [9] Dan Hendrycks, Steven Basart, Norman Mu, Saurav Kadavath, Frank Wang, Evan Dorundo, Rahul Desai, Tyler Zhu, Samyak Parajuli, Mike Guo, et al. The many faces of robustness: A critical analysis of out-of-distribution generalization. In *ICCV*, pages 8340–8349, 2021. [11](#)
- [10] Dan Hendrycks, Kevin Zhao, Steven Basart, Jacob Steinhardt, and Dawn Song. Natural adversarial examples. In *CVPR*, pages 15262–15271, 2021. [11](#)
- [11] Yan Huang, Shang Li, Liang Wang, Tieniu Tan, et al. Unfolding the alternating optimization for blind super resolution. *NeurIPS*, 33:5632–5643, 2020. [5](#)
- [12] Chao Jia, Yinfei Yang, Ye Xia, Yi-Ting Chen, Zarana Parekh, Hieu Pham, Quoc Le, Yun-Hsuan Sung, Zhen Li, and Tom Duerig. Scaling up visual and vision-language representation learning with noisy text supervision. In *ICML*, pages 4904–4916. PMLR, 2021. [1](#), [2](#), [3](#)
- [13] Menglin Jia, Luming Tang, Bor-Chun Chen, Claire Cardie, Serge Belongie, Bharath Hariharan, and Ser-Nam Lim. Visual prompt tuning. In *ECCV*, pages 709–727. Springer, 2022. [1](#), [4](#)
- [14] Baoshuo Kan, Teng Wang, Wenpeng Lu, Xiantong Zhen, Weili Guan, and Feng Zheng. Knowledge-aware prompt tuning for generalizable vision-language models. In *ICCV*, pages 15670–15680, 2023. [2](#)
- [15] Muhammad Uzair Khattak, Hanoona Rasheed, Muhammad Maaz, Salman Khan, and Fahad Shahbaz Khan. Maple: Multi-modal prompt learning. In *CVPR*, pages 19113–19122, 2023. [1](#), [2](#), [3](#), [4](#), [11](#)
- [16] Muhammad Uzair Khattak, Syed Talal Wasim, Muzammal Naseer, Salman Khan, Ming-Hsuan Yang, and Fahad Shahbaz Khan. Self-regulating prompts: Foundational model adaptation without forgetting. In *ICCV*, pages 15190–15200, 2023. [1](#), [2](#), [3](#), [4](#), [5](#), [6](#), [11](#)
- [17] Gahyeon Kim, Sohee Kim, and Seokju Lee. Aapl: Adding attributes to prompt learning for vision-language models. In *CVPR*, pages 1572–1582, 2024. [2](#)
- [18] Jonathan Krause, Michael Stark, Jia Deng, and Li Fei-Fei. 3d object representations for fine-grained categorization. In *ICCV workshop*, pages 554–561, 2013. [7](#), [11](#)
- [19] Nilakshan Kunanathaseelan, Jing Zhang, and Mehrtaash Harandi. Lavip: Language-grounded visual prompting. In *AAAI*, pages 2840–2848, 2024. [1](#)
- [20] Dongjun Lee, Seokwon Song, Jihee Suh, Joonmyeong Choi, Sanghyeok Lee, and Hyunwoo J Kim. Read-only prompt optimization for vision-language few-shot learning. In *ICCV*, pages 1401–1411, 2023. [2](#)
- [21] Brian Lester, Rami Al-Rfou, and Noah Constant. The power of scale for parameter-efficient prompt tuning. *arXiv preprint arXiv:2104.08691*, 2021. [1](#), [2](#)
- [22] Xiang Lisa Li and Percy Liang. Prefix-tuning: Optimizing continuous prompts for generation. *arXiv preprint arXiv:2101.00190*, 2021. [1](#), [2](#)
- [23] Zheng Li, Xiang Li, Lingfeng Yang, Borui Zhao, Renjie Song, Lei Luo, Jun Li, and Jian Yang. Curriculum temperature for knowledge distillation. In *AAAI*, pages 1504–1512, 2023. [5](#)
- [24] Zheng Li, Xiang Li, Xinyi Fu, Xin Zhang, Weiqiang Wang, Shuo Chen, and Jian Yang. Promptkd: Unsupervised prompt distillation for vision-language models. In *CVPR*, pages 26617–26626, 2024. [1](#), [2](#), [4](#), [5](#)
- [25] Hanxiao Liu, Karen Simonyan, and Yiming Yang. Darts: Differentiable architecture search. *arXiv preprint arXiv:1806.09055*, 2018. [5](#), [11](#)
- [26] Jiasen Lu, Dhruv Batra, Devi Parikh, and Stefan Lee. Vilbert: Pretraining task-agnostic visiolinguistic representations for vision-and-language tasks. *NeurIPS*, 32, 2019. [1](#)
- [27] Subhansu Maji, Esa Rahtu, Juho Kannala, Matthew Blaschko, and Andrea Vedaldi. Fine-grained visual classification of aircraft. *arXiv preprint arXiv:1306.5151*, 2013. [7](#), [11](#)

- [28] Sachit Menon and Carl Vondrick. Visual classification via description from large language models. *arXiv preprint arXiv:2210.07183*, 2022. [2](#)
- [29] Maria-Elena Nilsback and Andrew Zisserman. Automated flower classification over a large number of classes. In *2008 Sixth Indian conference on computer vision, graphics & image processing*, pages 722–729. IEEE, 2008. [7](#), [11](#)
- [30] Omkar M Parkhi, Andrea Vedaldi, Andrew Zisserman, and CV Jawahar. Cats and dogs. In *CVPR*, pages 3498–3505. IEEE, 2012. [7](#), [11](#)
- [31] Adam Paszke, Sam Gross, Francisco Massa, Adam Lerer, James Bradbury, Gregory Chanan, Trevor Killeen, Zeming Lin, Natalia Gimelshein, Luca Antiga, et al. Pytorch: An imperative style, high-performance deep learning library. In *NeurIPS*, pages 8026–8037, 2019. [11](#)
- [32] Hieu Pham, Melody Guan, Barret Zoph, Quoc Le, and Jeff Dean. Efficient neural architecture search via parameters sharing. In *ICML*, pages 4095–4104. PMLR, 2018. [5](#)
- [33] Alec Radford, Jong Wook Kim, Chris Hallacy, Aditya Ramesh, Gabriel Goh, Sandhini Agarwal, Girish Sastry, Amanda Askell, Pamela Mishkin, Jack Clark, et al. Learning transferable visual models from natural language supervision. In *ICML*, pages 8748–8763. PMLR, 2021. [1](#), [2](#), [3](#)
- [34] Benjamin Recht, Rebecca Roelofs, Ludwig Schmidt, and Vaishal Shankar. Do imagenet classifiers generalize to imagenet? In *ICML*, pages 5389–5400. PMLR, 2019. [11](#)
- [35] Shuvendu Roy and Ali Etamad. Consistency-guided prompt learning for vision-language models. *arXiv preprint arXiv:2306.01195*, 2023. [2](#)
- [36] Khurram Soomro, Amir Roshan Zamir, and Mubarak Shah. Ucf101: A dataset of 101 human actions classes from videos in the wild. *arXiv preprint arXiv:1212.0402*, 2012. [7](#), [11](#)
- [37] Zeyi Sun, Ye Fang, Tong Wu, Pan Zhang, Yuhang Zang, Shu Kong, Yuanjun Xiong, Dahua Lin, and Jiaqi Wang. Alpha-clip: A clip model focusing on wherever you want. In *CVPR*, pages 13019–13029, 2024. [1](#)
- [38] Hao Tan and Mohit Bansal. Lxmert: Learning cross-modality encoder representations from transformers. *arXiv preprint arXiv:1908.07490*, 2019. [1](#)
- [39] Xinyu Tian, Shu Zou, Zhaoyuan Yang, and Jing Zhang. Argue: Attribute-guided prompt tuning for vision-language models. In *CVPR*, pages 28578–28587, 2024. [2](#)
- [40] Haohan Wang, Songwei Ge, Zachary Lipton, and Eric P Xing. Learning robust global representations by penalizing local predictive power. *NeurIPS*, 32, 2019. [11](#)
- [41] Yubin Wang, Xinyang Jiang, De Cheng, Dongsheng Li, and Cairong Zhao. Learning hierarchical prompt with structured linguistic knowledge for vision-language models. In *AAAI*, pages 5749–5757, 2024. [2](#)
- [42] Jason Wei, Xuezhi Wang, Dale Schuurmans, Maarten Bosma, Fei Xia, Ed Chi, Quoc V Le, Denny Zhou, et al. Chain-of-thought prompting elicits reasoning in large language models. *NeurIPS*, 35:24824–24837, 2022. [5](#)
- [43] Ge Wu, Xin Zhang, Zheng Li, Zhaowei Chen, Jiajun Liang, Jian Yang, and Xiang Li. Cascade prompt learning for vision-language model adaptation. In *ECCV*, 2024. [1](#)
- [44] Jianxiong Xiao, James Hays, Krista A Ehinger, Aude Oliva, and Antonio Torralba. Sun database: Large-scale scene recognition from abbey to zoo. In *CVPR*, pages 3485–3492. IEEE, 2010. [7](#), [11](#)
- [45] Hantao Yao, Rui Zhang, and Changsheng Xu. Visual-language prompt tuning with knowledge-guided context optimization. In *CVPR*, pages 6757–6767, 2023. [2](#), [3](#), [11](#)
- [46] Yajing Zhai, Yawen Zeng, Zhiyong Huang, Zheng Qin, Xin Jin, and Da Cao. Multi-prompts learning with cross-modal alignment for attribute-based person re-identification. In *AAAI*, pages 6979–6987, 2024. [2](#)
- [47] Ji Zhang, Shihan Wu, Lianli Gao, Heng Tao Shen, and Jingkuan Song. Dept: Decoupled prompt tuning. In *CVPR*, pages 12924–12933, 2024. [1](#)
- [48] Denny Zhou, Nathanael Schärli, Le Hou, Jason Wei, Nathan Scales, Xuezhi Wang, Dale Schuurmans, Claire Cui, Olivier Bousquet, Quoc Le, et al. Least-to-most prompting enables complex reasoning in large language models. *arXiv preprint arXiv:2205.10625*, 2022. [5](#)
- [49] Kaiyang Zhou, Jingkang Yang, Chen Change Loy, and Ziwei Liu. Conditional prompt learning for vision-language models. In *CVPR*, pages 16816–16825, 2022. [1](#), [2](#), [3](#), [4](#), [5](#), [6](#), [11](#)
- [50] Kaiyang Zhou, Jingkang Yang, Chen Change Loy, and Ziwei Liu. Learning to prompt for vision-language models. *IJCV*, 130(9):2337–2348, 2022. [1](#), [2](#), [3](#), [4](#), [5](#), [6](#), [11](#)
- [51] Beier Zhu, Yulei Niu, Yucheng Han, Yue Wu, and Hanwang Zhang. Prompt-aligned gradient for prompt tuning. In *ICCV*, pages 15659–15669, 2023. [2](#), [3](#)
- [52] Barret Zoph, Vijay Vasudevan, Jonathon Shlens, and Quoc V Le. Learning transferable architectures for scalable image recognition. In *CVPR*, pages 8697–8710, 2018. [5](#)

ATPrompt: Textual Prompt Learning with Embedded Attributes

Supplementary Material

6. Implementation Details

6.1. Dataset

We evaluate the performance of our method on 15 recognition datasets. For generalization from base-to-novel classes and cross-dataset evaluation, we evaluate the performance of our method on 11 diverse recognition datasets. Specifically, these datasets include ImageNet-1K [6] and Caltech-101 [7] for generic object classification; OxfordPets [30], StanfordCars [18], Flowers102 [29], Food101 [3], and FGVCAircraft [27] for fine-grained classification, SUN-397 [44] for scene recognition, UCF-101 [36] for action recognition, DTD [5] for texture classification, and EuroSAT [8] for satellite imagery recognition. For domain generalization experiments, we use ImageNet-1K [6] as the source dataset and its four variants as target datasets including ImageNet-V2 [34], ImageNet-Sketch [40], ImageNet-A [10], and ImageNet-R [9].

6.2. Attribute Search

Inspired by DARTS [25], we utilize a differentiable search method to learn and select the appropriate attribute content and quantity for our proposed attribute-embedded form. During the search process, the batch size is set to 32, and the number of training epochs is set to 40. We use SGD as the optimizer for soft prompts θ , as shown in Eqn. (12), with an initial learning rate of 0.002. Additionally, we employ Adam as the optimizer for the weight vector α , as indicated in Eqn. (11), with an initial learning rate of 0.02. In our experiments, we configure the number of attribute bases to 5, resulting in the generation of 31 attribute combinations.

In Tab. 12, we present the five specific attribute bases obtained after querying the LLM, as well as the optimal attribute for training after searching. Tab. 13 displays the attributes and their corresponding weights from the final epoch of the search stage for the Caltech-101 dataset.

6.3. Base-to-Novel Generalization

Baseline Methods. We apply our ATPrompt to a wide range of textual-based prompt learning approaches, including CoOp [50], CoCoOp [49], KgCoOp [45], MaPLe [15], and PromptSRC [16].

Settings. Our code is implemented using PyTorch [31]. All experiments were conducted on a single NVIDIA V100 GPU. We adopted the standard data augmentation scheme as the baseline method, including random resized cropping and flipping. We employed stochastic gradient descent (SGD) as the optimizer. By default, we set the soft prompt lengths a_m , b_m , and M in Eqn. (4) to be the same,

as attribute and class tokens are considered equally important. The implementation details for each baseline method are presented as follows:

CoOp+ATPrompt: The experimental settings are consistent with the baseline method, with a batch size of 32 and an initial learning rate of 0.002. According to the original paper, the learnable prompt length M for ResNet-50 CLIP is reported as 16; however, detailed results for the ViT-B/16 CLIP were not provided. In our setup, we configured the learnable attribute prompt lengths a_m and b_m , as well as the learnable class prompt length M to be 2. The baseline model is trained for 200 epochs using cosine decay. In our approach, we train the model for 100 epochs while maintaining the same decay schedule. Fig. 6 illustrates the architectural comparison between the original CoOp and the CoOp+ATPrompt.

KgCoOp+ATPrompt: In accordance with the baseline method, we use a batch size of 128 and an initial learning rate of 0.002. The loss hyperparameter λ , as reported in the paper, is set at 8. However, given that our ATPrompt already exhibits a regularization effect, we reduce this hyperparameter to 2. We adhere to the same training schedule as the baseline method. A detailed architectural comparison between KgCoOp and KgCoOp+ATPrompt is presented in Fig. 6.

CoCoOp+ATPrompt: In line with the baseline method, we employ a batch size of 1 and an initial learning rate of 0.002. The original paper specifies a learnable class prompt length of 4. In contrast, our method sets the lengths of both the learnable attribute soft prompts, a_m and b_m , as well as the learnable class soft prompt, M , to 2. We follow the same training schedule as the baseline method, which involves training the model over 10 epochs using cosine decay.

In the original paper, CoCoOp introduces a meta network that processes image features to generate meta tokens, which serve as offsets for all soft prompt tokens. In our CoCoOp+ATPrompt, we maintain both the meta network and the meta tokens; however, the meta tokens are exclusively used as offsets for class soft tokens $[T_1], \dots, [T_M]$, as illustrated in Fig. 7.

MaPLe+ATPrompt: Following the baseline method, we use a batch size of 4 and an initial learning rate of 0.0035. While the original paper sets the length of the learnable prompt to 2, our approach involves setting the lengths of both the learnable attribute soft prompts, a_m and b_m , as well as the learnable class soft prompt, M , to 4. Our training schedule mirrors that of the baseline method.

According to the original paper, all textual soft tokens are input into the projection layer to acquire visual to-

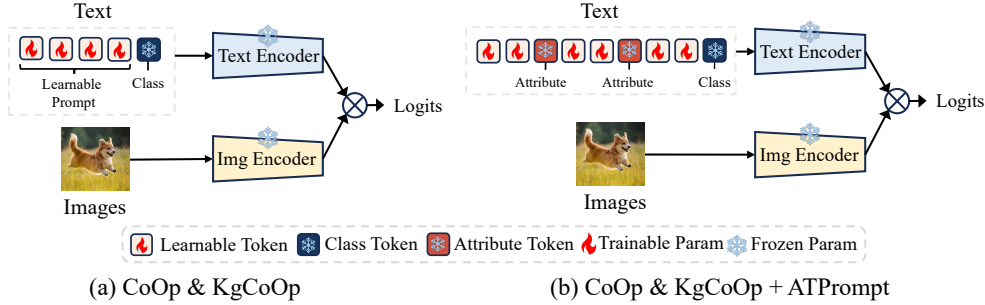


Figure 6. Architectural comparison between CoOp & KgCoOp and CoOp & KgCoOp + ATPrompt.

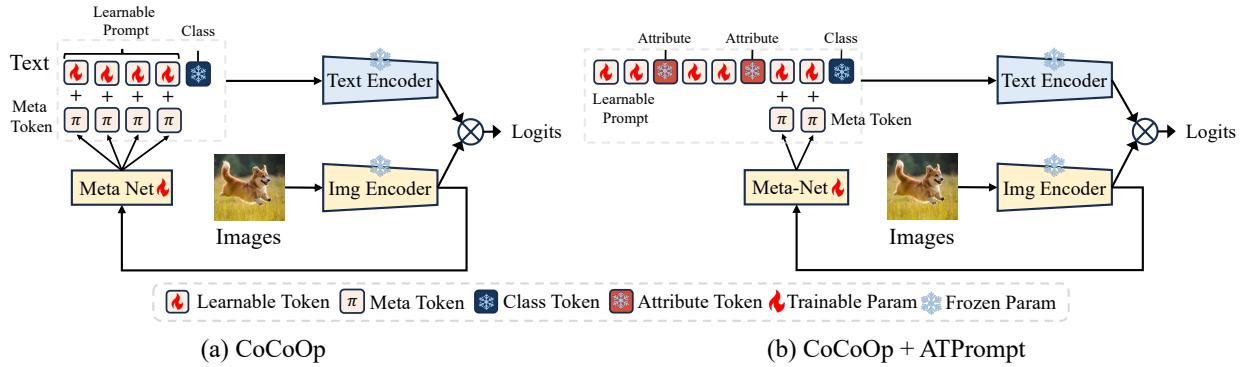


Figure 7. Architectural comparison between CoCoOp and CoCoOp+ATPrompt. In CoCoOp+ATPrompt, meta tokens are only added as offsets to class soft tokens.

Version	Method	Target Dataset						
		Source ImageNet	-V2	-S	-A	-R	Avg.	Δ
Shallow	CoOp	71.51	64.20	47.99	49.71	75.21	59.28	
	+ATPrompt	71.67	64.43	49.13	50.91	76.24	60.18	(+0.90)
Shallow	CoCoOp	71.02	64.07	48.75	50.63	76.18	59.91	
	+ATPrompt	71.27	64.66	49.15	51.44	76.33	60.40	(+0.49)
Deep	MaPLe	70.72	64.07	49.15	50.90	76.98	60.27	
	+ATPrompt	70.69	64.40	49.10	51.77	77.11	60.60	(+0.33)

Table 8. Domain generalization experiments of three baselines with and without our ATPrompt on 4 datasets. Our method achieves consistent average performance improvement over three baseline methods.

kens, which are subsequently inserted into the deeper layers of the image encoder. However, in MaPLe+ATPrompt, we only input class soft tokens into the projection layer and do not modify the attribute soft and hard tokens. A detailed architectural comparison between MaPLe and MaPLe+ATPrompt is illustrated in Fig. 8.

PromptSRC+ATPrompt: Similar to the baseline method, our approach uses a batch size of 4, an initial learning rate of 0.0025, a text loss weight of 25, and an image loss weight of 10. We adhere to the same training schedule as the baseline method. In the original study, the soft prompt length is specified as 4. In our approach, we set the lengths of both the learnable attribute prompts a_m and b_m , as well as the learnable class soft prompt M , to 4.

In our study, we exclusively remove and later reintroduce deep class soft tokens $[T_1]_i, \dots, [T_M]_i$, as explained in our paper. Meanwhile, attribute-related soft tokens $[T_{a_1}]_i, \dots, [T_{b_m}]_i$, along with hard tokens $[A]_i$ and $[B]_i$, are retained throughout the forward process. A comprehensive architectural comparison between PromptSRC and PromptSRC+ATPrompt is presented in Fig. 9.

7. Additional Experiments

7.1. Domain Generalization

Tab. 8 shows the domain generalization results for three baseline methods. The results show that our method improves CoOp, CoCoOp and MaPLe methods by 0.90%,

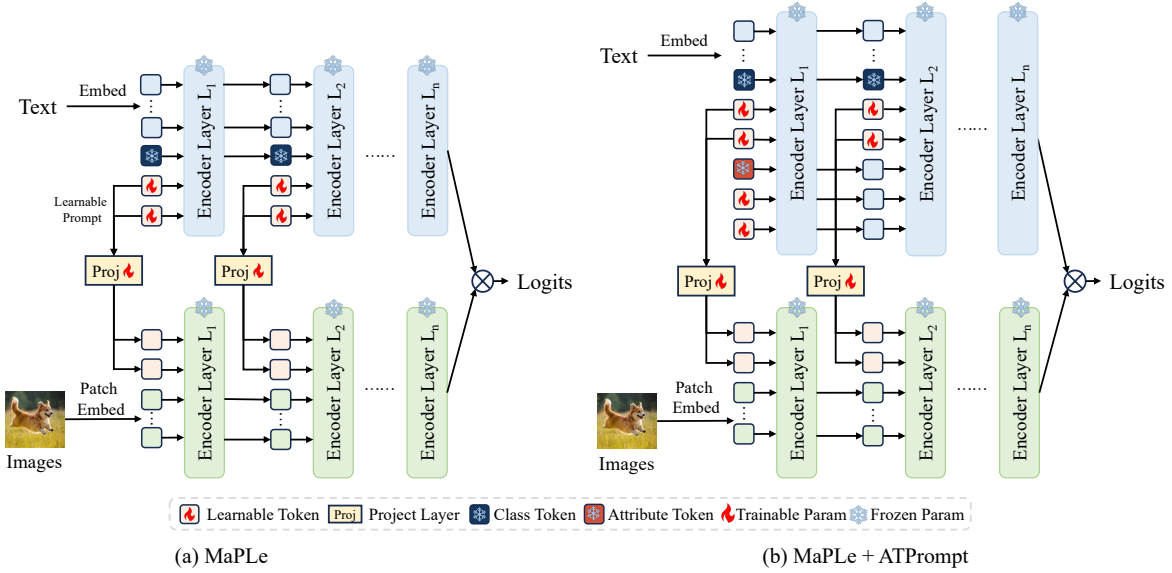


Figure 8. Architectural comparison between MaPLe and MaPLe+ATPrompt.

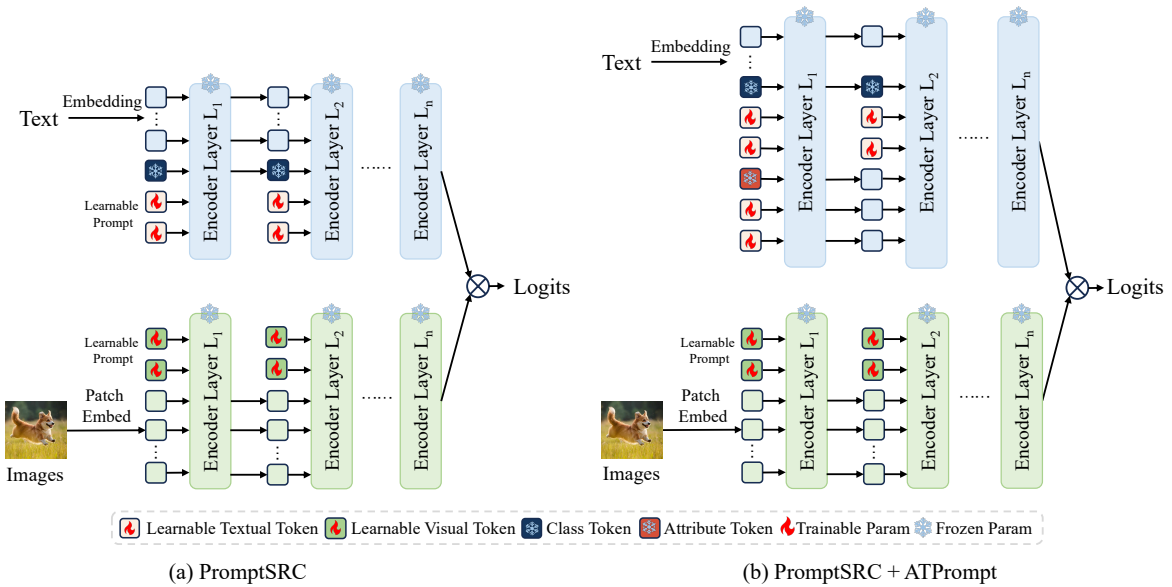


Figure 9. Architectural comparison between PromptSRC and PromptSRC+ATPrompt. In PromptSRC+ATPrompt, we only drop and reintroduce class soft tokens in the deep layers. The attribute soft and hard tokens are retained throughout the forward process.

0.49% and 0.33% respectively.

7.2. Ablation Study

Attribute Order. We have conducted some experiments in the main paper and verified that the order of attributes does not significantly impact model performance. The fluctuation of the results is within a reasonable range. Due to page limitations, we only provide a portion of the results in the main paper. In Tab. 9, we conduct more experiments to verify our observations.

Attribute Position. In addition to assessing the impact of

the class token’s position within the textual prompt on performance, we also examine the influence of the attribute token’s positioning. Fig. 10 and Tab. 10 present the visualization of attribute positions and the corresponding experimental results, respectively. The results indicate that the interval version achieves the best performance among all variations.

Initialization. Existing baseline methods initialize the soft tokens using the embeddings of the phrase “a photo of a” in their official implementations across 11 recognition datasets. However, in our approach, the addition of attribute tokens may render this initialization strategy inappropriate.

Attributes	Base	Novel	HM
(material, function)	76.40	70.13	73.13
(function, material)	76.28	70.00	73.01
(growth, season)	76.46	70.18	73.19
(season, growth)	76.40	70.21	73.17
(color, size, shape)	76.27	69.95	72.97
(shape, size, color)	76.32	70.19	73.13
(habitat, size, shape)	76.50	70.21	73.22
(habitat, shape, size)	76.46	70.08	73.13
Searched Attributes (color, shape)	76.27	70.60	73.33

Table 9. Comparison of different attribute orders on ImageNet. Changes in attribute order will not significantly affect model performance.

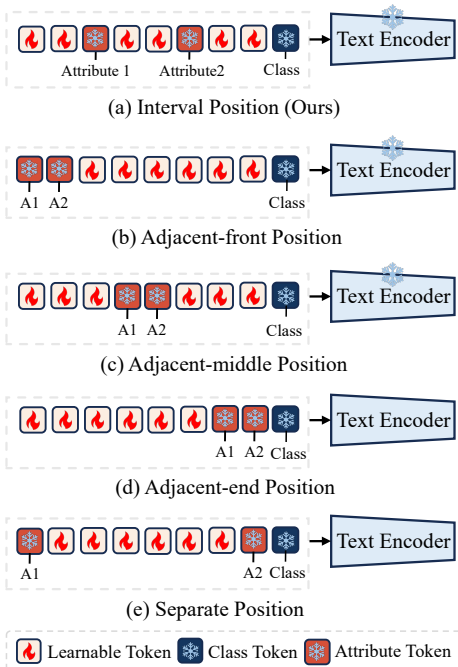


Figure 10. Comparison of attribute tokens at different positions, taking two attributes as an example.

Version	Base	Novel	HM
Baseline (CoOp)	76.47	67.88	71.92
(a) Interval (Ours)	76.27	70.60	73.33
(b) Adjacent-front	76.39	70.22	73.18
(c) Adjacent-middle	76.46	70.11	73.15
(d) Adjacent-end	76.34	70.31	73.20
(e) Separate	76.48	70.08	73.14

Table 10. Performance results of attribute tokens at different positions in ATPrompt on ImageNet. The interval version achieves best results.

Attribute	Base	Novel	HM
“a photo of a”	76.40	70.07	73.10
Random Normal Init	76.27	70.60	73.33

Table 11. Comparison of different initialization ways on ImageNet. Random normal initialization performs better.

In our method, the class soft tokens $[T_1], \dots, [T_M]$ are randomly initialized by sampling from a zero-mean Gaussian distribution with a standard deviation of 0.02. In Tab. 11, we compare the effects of different initialization methods on model performance. Experimental results show that random initialization provides a superior starting point for training.

8. Discussion

8.1. Comparison with Querying LLM Directly.

There are two disadvantages to directly asking a large language model to obtain universal attributes. First, determining the optimal content of these attributes is challenging. Second, identifying the ideal number of attributes is equally difficult. However, if a user wishes to acquire attributes directly in this manner, it remains a feasible approach. Our experiments have shown that the optimal number of attributes is often around two. Therefore, if the user prefers to avoid the attribute search process, directly asking the language model to summarize two universal attributes for known categories and then using them for training is a more convenient method, albeit at the cost of some performance.

9. Limitations and Future Works.

(1) Our proposed approach utilizes a differentiable search method that learns to identify suitable attributes for our prompt format. While this method avoids lengthy training times and high costs, there is still room for optimization. We attempted to employ a Large Language Model (LLM) to discover suitable attributes, but determining the optimal number of attributes for the current format remains a challenge. In future research, we plan to investigate how to leverage the Chain-of-Thought (CoT) method to further explore the potential of Multimodal Large Language Models (MLLM) in enhancing the attribute discovery process. (2) Our approach involves embedding fixed explicit attributes into soft prompts to enhance model performance. In the future, we intend to explore transitioning from using explicit fixed attributes to implicit, learnable attributes. This shift aims to enable the model to autonomously discover suitable attributes in a learning-driven manner, thereby improving model performance.

Dataset	Attribute Bases	Searched Attributes
ImageNet-1K	color, size, shape, habitat, behavior	(color, shape)
Caltech-101	shape, color, material, function, size	(shape,size)
Oxford Pets	loyalty, affection, playfulness, energy, intelligence	(playfulness, energy)
Stanford Cars	design, engine, performance, luxury, color	(luxury)
Flowers-102	color, flower, habitat, growth, season	(color, habitat, growth)
Food-101	flavor, texture, origin, ingredients, preparation	(flavor, preparation)
FGVC Aircraft	design, capacity, range, engines, liveries	(design, range)
SUN-397	architecture, environment, structure, design, function	(function)
DTD	pattern, texture, color, design, structure	(pattern, color, design)
EuroSAT	habitat, foliage, infrastructure, terrain, watercourse	(habitat)
UCF-101	precision, coordination, technique, strength, control	(precision)

Table 12. Attribute bases and searched results for each dataset.

Attributes	shape, color, material, function, size
Combinations & Weights	(shape), score: 0.298
	(color), score: 0.004
	(material), score: 0.002
	(function), score: 0.002
	(size), score: 0.003
	(shape, color), score: 0.003
	(shape, material), score: 0.006
	(shape, function), score: 0.000
	(shape, size), score: 0.565
	(color, material), score: 0.000
	(color, function), score: 0.001
	(color, size), score: 0.005
	(material, function), score: 0.000
	(material, size), score: 0.002
	(function, size), score: 0.002
	(shape, color, material), score: 0.002
	(shape, color, function), score: 0.002
	(shape, color, size), score: 0.000
	(shape, material, function), score: 0.001
	(shape, material, size), score: 0.085
	(shape, function, size), score: 0.001
	(color, material, function), score: 0.001
	(color, material, size), score: 0.000
	(color, function, size), score: 0.002
	(material, function, size), score: 0.001
(shape, color, material, function), score: 0.001	
(shape, color, material, size), score: 0.001	
(shape, color, function, size), score: 0.001	
(shape, material, function, size), score: 0.005	
(color, material, function, size), score: 0.001	
(shape, color, material, function, size), score: 0.001	

Table 13. Output results after 40 epochs of training on Caltech101.